

DMD # 086322

Title Page

Title

Modeling of hepatic drug metabolism and responses in CYP2C19 poor metabolizer using genetically manipulated human iPS cells

Authors & Affiliations

Sayaka Deguchi,

Tomoki Yamashita,

Keisuke Igai,

Kazuo Harada,

Yukiko Toba,

Kazumasa Hirata,

Kazuo Takayama, email: takayama@phs.osaka-u.ac.jp

Hiroyuki Mizuguchi, email: mizuguch@phs.osaka-u.ac.jp

Laboratory of Biochemistry and Molecular Biology, Graduate School of Pharmaceutical Sciences, Osaka University, Osaka 565-0871, Japan (S.D., T.Y., K.I., Y.T., K.T., H.M.)

Laboratory of Applied Environmental Biology, Graduate School of Pharmaceutical Sciences, Osaka University, Osaka 565-0871, Japan (K.Harada, K.Hirata)

PRESTO, Japan Science and Technology Agency, Saitama 332-0012, Japan (K.T.)

Laboratory of Hepatocyte Regulation, National Institutes of Biomedical Innovation,

DMD # 086322

Health and Nutrition, Osaka 567-0085, Japan (Y.T., K.T., H.M.)

Global Center for Medical Engineering and Informatics, Osaka University, Osaka 565-
0871, Japan (H.M.)

DMD # 086322

Running Title Page

Modeling of CYP2C19 PM using genome-edited hiPSCs

Corresponding authors

Dr. Kazuo Takayama

Laboratory of Biochemistry and Molecular Biology, Graduate School of Pharmaceutical Sciences, Osaka University, 1-6 Yamadaoka, Suita, Osaka 565-0871, Japan.

Phone: +81-6-6879-8187

FAX: +81-6-6879-8187

E-mail: takayama@phs.osaka-u.ac.jp

Dr. Hiroyuki Mizuguchi

Laboratory of Biochemistry and Molecular Biology, Graduate School of Pharmaceutical Sciences, Osaka University, 1-6 Yamadaoka, Suita, Osaka 565-0871, Japan.

Phone: +81-6-6879-8185

FAX: +81-6-6879-8187

E-mail: mizuguch@phs.osaka-u.ac.jp

text pages: 31

tables: 0

DMD # 086322

figures: 7

references: 21

words in the Abstract: 247

words in the Introduction: 477

words in the Discussion: 503

List of Abbreviations

AAT: alpha-1 antitrypsin

AFP: alpha-fetoprotein

ALB: albumin

BMP: bone morphogenetic protein

CES1: carboxylesterase 1

CRISPR/Cas9: clustered-regularly-interspaced-short-palindromic-repeats/CRISPR-associated 9

CYP: cytochrome P450

CYP2C19-KO HLCs: CYP2C19-knockout human iPS cell-derived hepatocyte-like cells

DMSO: dimethyl sulfoxide

EF1 α promoter: elongation factor 1 alpha promoter

EGF: epidermal growth factor

GAPDH: glyceraldehyde 3-phosphate dehydrogenase

GEO: gene expression omnibus

GO: gene ontology

DMD # 086322

GWAS: genome-wide association study

HCM: hepatocyte culture medium

HGF: hepatocyte growth factor

HLCs: hepatocyte-like cells

HNF4A: hepatocyte nuclear factor 4 alpha

human iPS cells: human induced pluripotent stem cells

MPS: microphysiological system

MRM: multiple-reaction monitoring

OsM: oncostatin M

pA: polyadenylation sequence

PHHs: primary human hepatocytes

PM: poor metabolizer

PuroR: puromycin resistant protein

SNP: single nucleotide polymorphism

TTR: transthyretin

WT: wild type

WT HLCs: wild type iPS cell-derived hepatocyte-like cells

DMD # 086322

Abstract

Cytochrome P450 family 2 subfamily C member 19 (CYP2C19), in liver, plays important roles in terms of drug metabolism. It is known that CYP2C19 poor metabolizers (PMs) lack CYP2C19 metabolic capacity. Thus, unexpected drug-induced liver injury or decrease of drug efficacy would be caused in CYP2C19 substrate-treated CYP2C19 PMs. However, it is difficult to evaluate the safety and effectiveness of drugs and candidate compounds for CYP2C19 PMs because there is currently no model for this phenotype. Here, using human iPS cells and our highly efficient genome editing and hepatocyte differentiation technologies, we generated CYP2C19-knockout human iPS cell-derived hepatocyte-like cells (CYP2C19-KO HLCs) as a novel CYP2C19 PM model for drug development and research. The gene expression levels of hepatocyte markers were similar between WT HLCs and CYP2C19-KO HLCs, suggesting that CYP2C19 deficiency did not affect the hepatic differentiation potency. We also examined CYP2C19 metabolic activity by measuring *S*-mephenytoin metabolites using LC-MS. The CYP2C19 metabolic activity was almost eliminated by CYP2C19 knockout. Additionally, we evaluated whether clopidogrel (CYP2C19 substrate)-induced liver toxicity could be predicted using our model. Unexpectedly, there was no significant difference in cell viability between clopidogrel-treated WT HLCs and CYP2C19-KO HLCs. However, the cell viability in clopidogrel- and ketoconazole (CYP3A4 inhibitor)-treated CYP2C19-KO HLCs was significantly enhanced as compared with that in clopidogrel- and DMSO-treated CYP2C19-KO HLCs. This result suggests that CYP2C19-KO HLCs can predict the clopidogrel-induced liver toxicity. We succeeded in generating CYP2C19 PM model

DMD # 086322

cells using human iPS cells and genome editing technologies for pharmaceutical research.

Significance Statement

Although unexpected drug-induced liver injury or decrease of drug efficacy would be caused in CYP2C19 substrate-treated CYP2C19 poor metabolizers, it is difficult to evaluate the safety and effectiveness of drugs and candidate compounds for CYP2C19 poor metabolizers because there is currently no model for this phenotype. Using human iPS cells and our highly efficient genome editing and hepatocyte differentiation technologies, we generated CYP2C19-knockout human iPS cell-derived hepatocyte-like cells as a novel CYP2C19 poor metabolizer model for drug development and research.

DMD # 086322

Introduction

The liver plays an essential role in drug metabolism. Drugs are metabolized in the liver, and transformed into active (or inactive) metabolites. Some drugs and their metabolites can cause hepatocellular toxicity (Macdonald and Robertson, 2009), compelling pharmaceutical companies to discontinue development of these drugs or withdraw them from the market. Therefore, establishment of the highly specific *in vitro* systems for the evaluation of drug metabolism and toxicity is a pressing issue.

Poor metabolizers (PMs) are individuals who lack of metabolic capacity of a specific drug metabolizing enzyme. Therefore, the plasma drug concentrations and frequency of side effects differ greatly between PMs and non-PMs (Stingl *et al.*, 2013). Because cytochrome P450 family 2 subfamily C member 19 (CYP2C19) largely contributes to the phase I reaction of drug metabolism (Zanger and Schwab, 2013), there is a concern that the PMs of CYP2C19 (CYP2C19-PMs) would suffer from the unexpected changes of pharmacokinetics and toxicity of CYP2C19 substrate drugs. Additionally, the frequency of CYP2C19-PMs is only 2 % in Caucasians but 18~23 % in Asians (Nakamura *et al.*, 1985; Bertilsson, 1995; Gardiner and Begg, 2006; Isomura *et al.*, 2010). For these reasons, to ensure the safety of drugs on the international market, we must develop a drug metabolism and toxicity evaluation system which considers CYP2C19-PMs and its ethnic differences. However, the available sources of primary human hepatocytes (PHHs), which are widely used in hepatocellular toxicity evaluation tests, are almost entirely limited to Caucasians, making it difficult to perform drug screening for CYP2C19-PMs.

DMD # 086322

In recent years, genome editing technologies using human induced pluripotent stem (iPS) cells have progressed rapidly. If we could use these technologies to establish CYP2C19-knockout human iPS cell-derived hepatocyte like cells (CYP2C19-KO HLCs), these cells could be used to reproduce the drug metabolism in CYP2C19-PMs. However, the genome editing efficiency depends on the target genes—that is, most of the transcriptionally inactive heterochromatic genes in undifferentiated iPS cells, including CYP2C19, can scarcely be edited (the biallelic-targeting efficiency is no more than 1 %). Therefore, we have optimized the conditions of the genome editing strategy and successfully enhanced the biallelic-targeting efficiency to more than 15 % by using RAD51-expressing plasmid and valproic acid (Takayama *et al.*, 2017). Moreover, we have developed an efficient hepatic differentiation protocol from human iPS cells (Takayama and Mizuguchi, 2017). From the above, we aimed to knockout the CYP2C19 gene using our unique genome editing technology in human iPS cells, and to differentiate the cells into HLCs so as to develop a cell culture system imitating CYP2C19-PMs.

In this study, we have established CYP2C19-KO iPS cells using a CRISPR-Cas9 system with several modifications. We then differentiated the CYP2C19-KO iPS cells into HLCs (CYP2C19-KO HLCs), which could be used as a hepatocyte model of CYP2C19-PMs. To evaluate whether the generated CYP2C19-KO HLCs would be useful for drug toxicity tests, we examined their response to CYP2C19 substrate drugs.

DMD # 086322

Materials and Methods

Human iPS cells

In this report, the human iPS cell line, FCL-iPS, was used. This iPS cell line was generated from PHHs, and the details are available in our previous report (Takayama *et al.*, 2014). The cells were maintained on iMatrix-511 (Nippi)-coated plates with StemFit AK02N medium (Ajinomoto) according to the manufacture's instructions.

Hepatic differentiation

Human iPS cells were dissociated into single cells using TrypLE Select Enzyme (Thermo Fisher Scientific) and plated onto Matrigel Basement Membrane Matrix, Growth Factor Reduced (Corning)-coated plate (MultiWell Plate for Cell/Tissue Culture 12F with lid, Sumitomo Bakelite). The cells were then cultured with StemFit AK02N medium for several days prior to the hepatic differentiation. When they reached approximately 80% confluence, the 4-step hepatic differentiation protocol was conducted. The first step is the induction of definitive endoderm (DE) cells, which is 4-days culture of human iPS cells in RPMI1640 medium (Sigma) containing 1×GlutaMAX (Thermo Fisher Scientific), 1×B27 Supplement Minus Vitamin A (Thermo Fisher Scientific), and 100 ng/ml Activin A (R&D Systems). The second step is the induction of hepatoblast-like cells, which is 5-days culture of the DE cells in RPMI1640 medium containing 1×GlutaMAX, 1×B27 Supplement Minus Vitamin A, 20 ng/ml bone morphogenetic protein (BMP) 4 (R&D Systems), and 20 ng/ml FGF4 (R&D Systems). The third step is the induction of HLCs, which is 5-days culture of the hepatoblast-like cells in RPMI1640 medium containing 1×GlutaMAX, 1×B27 Supplement Minus Vitamin A, and 20 ng/ml

DMD # 086322

hepatocyte growth factor (HGF, R&D Systems). The fourth step is the maturation of HLCs, which is 11-days culture of the HLCs in Hepatocyte Culture Medium (HCM, Lonza) without epidermal growth factor (EGF) but with 20 ng/ml oncostatin M (OsM, R&D Systems).

Real-time RT-PCR

By using ISOGEN (NIPPON GENE), total RNA was isolated from the cells. Using 500 ng of the isolated total RNA, cDNA was synthesized with a Superscript VILO cDNA synthesis kit (Thermo Fisher Scientific). Real-time RT-PCR was performed with SYBR Green PCR Master Mix (Applied Biosystems) using a StepOnePlus real-time PCR system (Applied Biosystems). The $2^{-\Delta\Delta CT}$ method was adopted for the relative quantitation of target mRNA levels. Namely, the values of the target genes were normalized by those of the housekeeping gene, *glyceraldehyde 3-phosphate dehydrogenase (GAPDH)*. PCR primer sequences (described in **Supplemental Table 1**) used in this report were obtained from PrimerBank (<https://pga.mgh.harvard.edu/primerbank/>).

Albumin secretion

To evaluate the albumin (ALB) secretion capacity of the cells, the culture supernatants, which were incubated for 24 hr after the medium was added, were collected. The collected supernatants were analyzed by ELISA with Human Albumin ELISA Quantitation Set (Bethyl Laboratories). ELISA was performed according to the manufacturer's instructions. The amount of ALB secretion was normalized by the protein content per well, which is evaluated with Pierce BCA Protein Assay Kit (Thermo Fisher

DMD # 086322

Scientific).

Immunohistochemistry

The human iPS cells and their derivatives were fixed with 4% paraformaldehyde in PBS at 4°C for 15 min. After blocking the cells with PBS containing 2% bovine serum albumin and 0.2% Triton X-100 at room temperature for 45 min, the cells were incubated with a primary antibody at 4°C overnight, and then with a secondary antibody at room temperature for 1 hr. All the antibody used in this report are described in **Supplemental Table 2**.

DNA microarray

By using RNeasy Mini Kit (QIAGEN), total RNA was isolated from human iPS cell-derived HLCs. Then, all the operations related to the microarray, cDNA amplification, labeling, hybridization, and analysis were performed at TAKARA BIO INC. The platform of the microarray was SurePrint G3 Human Gene Expression 8x60K v3 (Agilent Technologies). The data is available at Gene Expression Omnibus (GEO), and its accession number is GSE123937. Gene Ontology (GO) enrichment clustering analysis was performed by using DAVID Bioinformatics Resources 6.8 (<https://david.ncifcrf.gov/>).

CYP2C19 and CYP3A4 activity

To examine the CYP2C19 and CYP3A4 activity, the UPLC-MS/MS analysis was performed. Human iPS cell-derived HLCs were cultured with medium containing 50 µM of *S*-mephenytoin (Toronto Research Chemicals, a substrate whose metabolite is 4'-hydroxymephenytoin) or 5 µM of midazolam (FUJIFILM Wako, a substrate whose

DMD # 086322

metabolite is 1'-hydroxymidazolam). The supernatant was collected at 24 hr after the treatment with the substrate. The collected supernatant was immediately mixed with two volumes of acetonitrile (FUJIFILM Wako). Samples were filtrated with AcroPrep Advance 96-Well Filter Plates (Pall Corporation) for 5 min at 1,750 g, and then the supernatant was analyzed by UPLC-MS/MS to measure the concentration of the metabolite according to the standard curve. UPLC analysis was performed using an Acquity UPLC (Waters) and MS/MS was performed on a Q-Premier XE (Waters). The mass spectrometer was set to the multiple-reaction monitoring (MRM) mode and was operated with the electrospray ionization source in positive ion mode. The MRM transition (m/z of precursor ion / m/z of product ion) for 4'-hydroxymephenytoin and 1'-hydroxymidazolam was 342.2/203.1 and 342.2/203.1, respectively. For transition, the cone voltage and collision energy were set at 40 V and 26 eV, respectively. The dwell time for each MRM transition was set at 100 milliseconds. LC separations were carried out at 40 °C with an Acquity UPLC BEH C18 column, 1.7 μ m, 2.1 X 50 mm (Waters). The mobile phase was delivered at a flow rate of 0.5 ml/min using a gradient elution profile consisting of solvent A (0.1% formic acid/distilled water) and solvent B (0.1% formic acid/acetonitrile). The initial composition of the binary solvent was 10% B from 0 to 0.5 min. Solvent B was increased from 10% to 100% over 2.0 min. The composition of solvent remained for 1.0 min at 100% B. Ten μ l of sample solution was injected into the column. The concentrations of the metabolite were calculated according to the standard followed by normalization to the protein content per well.

Cell viability

DMD # 086322

The cell viability of WT and CYP2C19-KO HLCs was assessed by WST-8 assay after 48 hr exposure to different concentrations of clopidogrel (0, 100, and 300 μM) in the presence or absence of the CYP3A4 inhibitor, ketoconazole (10 μM) and CYP2C19 inhibitor, N-3-Benzyl-nirvanol (1 μM). A Cell Counting Kit-8 was purchased from DOJINDO LABORATORIES. WST-8 assay was performed according to the manufacturer's instructions. The cell viability was calculated as a percentage of that in the cells treated with vehicle (DMSO) only.

Primary human hepatocytes (PHH)

Three lots of cryopreserved human hepatocytes (lots YOW, OHO, and FCL; Veritas) were used. The average values of the three lots were showed as "PHH" in this report. The vials of hepatocytes were rapidly thawed in a shaking water bath at 37°C; the contents of each vial were emptied into prewarmed Cryopreserved Hepatocyte Recovery Medium (CHRM; Thermo Fisher Scientific) and the suspension was centrifuged at 900 rpm for 10 min at room temperature. The hepatocytes were seeded at 1.25×10^5 cells/cm² in HCM containing 10% fetal calf serum (FCS, GIBCO) onto type I collagen-coated 12-well plates. The medium was replaced with HCM 6 hr after seeding. The hepatocytes, which were cultured 48 hr after plating the cells, were used in the experiments.

DMD # 086322

Results

Generation of CYP2C19-knockout human iPS cells

To establish CYP2C19-KO iPS cells, we designed donor plasmids targeting CYP2C19 (**Fig. 1A**). To efficiently perform the homologous recombination-mediated gene editing at the *CYP2C19* locus in human iPS cells, we used sgRNA/Cas9 co-expressing plasmids (pX330 (Le *et al.*, 2013)) and RAD51-expressing plasmids with donor plasmids. Human iPS cells were electroporated with these three plasmids. After the positive selection with puromycin, we isolated 24 single cell-derived colonies. To examine whether single cell-derived human iPS cells carry the transgene cassette at the targeted locus, genomic DNA was extracted and genotyping analysis was performed using the primers indicated by arrows in **figure 1A**. PCR primers were designed to distinguish wild type (WT) and mutant alleles; WT cells show a 2,750 bp band, biallelically-targeted cells show a 5,000 bp band and monoallelically-targeted cells show the two bands (a 2,750 bp and a 5,000 bp band). As shown in **figure 1B**, “clone 3” shows integration of the transgene into both alleles of *CYP2C19*. From this result, we could successfully establish the human iPS cells with a defect in exon 1 of the *CYP2C19* gene, which includes its start codon (CYP2C19-KO iPS cells).

Effect of CYP2C19 deficiency on the undifferentiated state

To characterize the effect of CYP2C19 deficiency on the undifferentiated state, we performed several assays (**Fig. 2**). Phase images showed that there was no morphological difference between WT iPS cells and CYP2C19-KO iPS cells (**Fig. 2A**). Real-time RT-PCR analysis showed that there was no significant difference in gene

DMD # 086322

expression levels of pluripotent markers (*NANOG*, *OCT3/4*, and *SOX2*) between the two groups (**Fig. 2B**). Immunostaining analysis also showed that there was no significant difference in the protein expression levels of OCT3/4 and SOX2 between the two groups (**Fig. 2C**). Taken together, these results suggested that CYP2C19 deficiency does not affect the undifferentiated state of human iPS cells.

Hepatic differentiation of CYP2C19-knockout human iPS cells

To examine whether the hepatic differentiation capacity of CYP2C19-KO iPS cells is similar to that of WT iPS cells, both WT iPS cells and CYP2C19-KO iPS cells were differentiated into HLCs as described in **figure 3A**, and then the gene expression levels of hepatic markers in WT HLCs and CYP2C19-KO HLCs were analyzed (**Fig. 3B**). The gene expression levels of *albumin (ALB)*, *alpha-fetoprotein (AFP)*, *alpha-1 antitrypsin (AAT)*, *transthyretin (TTR)*, *hepatocyte nuclear factor 4 alpha (HNF4A)*, and *CYP3A4* in CYP2C19-KO HLCs were similar to those in the WT HLCs. ELISA analysis showed that there were no significant differences in the ALB secretion capacity between WT HLCs and CYP2C19-KO HLCs (**Fig. 3C**). Immunostaining analysis also showed that there was no significant difference in the protein expression levels of ALB and AAT between WT HLCs and CYP2C19-KO HLCs (**Fig. 3D**). These results suggest that CYP2C19 deficiency does not affect the hepatic differentiation capacity of human iPS cells.

To characterize the global gene expression profiles in WT HLCs and CYP2C19-KO HLCs, microarray analysis was performed. This result shows that the gene expression of *CYP2C19* was almost entirely eliminated in CYP2C19-KO HLCs (**Fig. 4**,

DMD # 086322

shown in red letters). There was little difference in the gene expression levels of most genes (>99%) between WT HLCs and CYP2C19-KO HLCs (**Fig. 4**, shown in black dots). In addition, we extracted the 134 genes whose expression levels were up- or down-regulated more than 3-fold and analyzed them by the GO enrichment clustering analysis. As shown in **Supplemental Table 3**, the top GO cluster—i.e., the cluster with the highest enrichment score—indicated that the 134 genes may not affect either hepatic differentiation or metabolic capacity. Furthermore, the gene expression levels of other CYP2 forms were not changed by knockout of CYP2C19 (**Supplemental Figure 1**). We also confirmed that the expression levels of 231 genes that had the highest potential for off-target cleavage were not largely changed (**Supplemental Figure 2**). These results suggest that the specific genome editing of the *CYP2C19* locus was successfully accomplished by our strategy.

Drug metabolism capacity of CYP2C19-knockout human iPS cell-derived hepatocyte-like cells

To determine whether CYP2C19-KO HLCs have a defect in the drug metabolism capacity of CYP2C19, UPLC-MS/MS was performed (**Fig. 5**). The WT HLCs and CYP2C19-KO HLCs were treated with the *S*-mephenytoin, which is known to be a substrate of CYP2C19, and the amount of 4'-hydroxymephenytoin, which is the metabolite of *S*-mephenytoin, was measured by UPLC-MS/MS analysis. The metabolic activity in CYP2C19-KO HLCs was significantly lower than that in WT HLCs (WT HLCs = 4408.4 pg/mL/min/mg protein, CYP2C19-KO HLCs = below the limit of detection). This result indicates that CYP2C19-KO HLCs defect the drug metabolism

DMD # 086322

capacity of CYP2C19.

Drug response of CYP2C19-knockout human iPS cell-derived hepatocyte-like cells

Clopidogrel, a platelet aggregation inhibitor, is a prodrug that is metabolized into an active metabolite mainly by CYP2C19 (Wallentin *et al.*, 2010; Gillette *et al.*, 2016; Kiss *et al.*, 2018). In a study using primary rat hepatocytes and HepG2 cells, Zhai *et al.* revealed that the hepatocellular toxicity of clopidogrel is associated with the CYP2C19-mediated metabolism (Zhai *et al.*, 2016). Therefore, we expected that CYP2C19-KO HLCs would exhibit a different response to clopidogrel as compared with WT HLCs. To examine this, we treated WT HLCs and CYP2C19-KO HLCs with clopidogrel, and measured the cell viability 48 hr later (**Fig. 6**). Contrary to our expectation, the cell viabilities of CYP2C19-KO HLCs decreased in a dose-dependent manner as well as WT HLCs. This result suggests that not only CYP2C19 but also other drug metabolizing enzymes might contribute to the metabolism and toxicity of clopidogrel.

Drug response of ketoconazole-treated CYP2C19-knockout human iPS cell-derived hepatocyte-like cells

The results in **figure 6** suggest the existence of other drug metabolizing enzymes that contribute to the metabolism of clopidogrel, in addition to CYP2C19. Using the hepatoma cell line HepG2, Zahno *et al.* previously demonstrated that high CYP3A4 activity may be a risk factors for clopidogrel-associated hepatocellular toxicity (Zahno *et al.*, 2013). From these facts, we expected that CYP3A4 metabolizes clopidogrel into a hepatotoxic metabolite. To inhibit the CYP3A4 activity, we treated WT HLCs and CYP2C19-KO HLCs with ketoconazole, a CYP3A4 inhibitor, and assessed the cell

DMD # 086322

viability after 48 hr of clopidogrel-treatment (**Fig. 7**). As shown in **figure 7A**, the cell viabilities of both ketoconazole-treated WT HLCs and non-treated WT HLCs similarly decreased in a dose-dependent manner. However, the cell viability of ketoconazole-treated CYP2C19-KO HLCs was significantly higher than that of non-treated CYP2C19-KO HLCs (**Fig. 7B**). Taken together, these results suggest that the hepatocellular toxicity of clopidogrel can be predicted by using CYP2C19-KO HLCs in the presence of ketoconazole.

We also examined whether similar results could be obtained using selective inhibitors of CYP3A4 and CYP2C19. WT HLCs were treated with both ketoconazole (CYP3A4 inhibitor) and N-3-Benzyl-nirvanol (Suzuki *et al.*, 2002) (CYP2C19 inhibitor) followed by clopidogrel treatment, and then the cell viability was examined (**Supplemental Figure 3**). However, the cell viability was not enhanced by using these inhibitors. This result might be because N-3-Benzyl-nirvanol-mediated inhibition level of CYP2C19 activity was quite low (approximately 50%) (**Supplemental Figure 4**). As shown here, it is difficult to synthesis highly-selective CYP inhibitor, thus our CYP-KO HLCs might be an useful model for PM.

DMD # 086322

Discussion

In this study, we established CYP2C19-KO iPS cells using our unique and highly efficient genome editing technology. By differentiating the human iPS cells into HLCs, we obtained CYP2C19-KO HLCs. The CYP2C19 metabolic capacity decreased to below the limit of detection by deleting CYP2C19. The clopidogrel-induced hepatotoxicity test revealed a significant difference between the cell viability of WT HLCs and that of CYP2C19-KO HLCs in the presence or absence of ketoconazole. These results indicated that our CYP2C19-KO HLCs could be useful model cells for predicting the CYP2C19-mediated hepatocellular toxicity.

In general, clopidogrel is administered orally. After oral administration, 85 % of clopidogrel is hydrolyzed at the intestine into inactive metabolites by carboxylesterase 1 (CES1) and excreted, and the residual 15 % reaches the liver and is there metabolized into active metabolites by CYPs (Simon *et al.*, 2009; Kahma *et al.*, 2018). Therefore, to perform a more specific pharmacokinetics study of orally administered drugs such as clopidogrel, a combined model consisting of hepatocytes and intestinal enterocytes will be needed. One such cell model has already been reported: a microphysiological system (MPS) using PHHs as hepatocytes and Caco-2 cells as intestinal enterocytes (Tsamandouras *et al.*, 2017). By applying this technology, it is anticipated that an MPS consisting of enterocyte-like cells and HLCs, both of which are differentiated from the same individual-derived human iPS cells (e.g., CYP2C19-PM iPS cells), will be established in the new future. In other words, we can create an isogenic intestine and liver systems by using our CYP2C19-KO iPS cells, which would help us to predict the

DMD # 086322

bioavailability of orally administered drugs in CYP2C19-PM individuals. Such a system would make a substantial contribution to the field of personalized medicine.

In addition to CYP2C19-PMs, CYP2C9-PMs or CYP2D6-PMs have also been reported (Gardiner and Begg, 2006). By adopting the technology that we showed in this report, it would be possible to obtain these PM model HLCs. Using these cells, it is expected to establish the diverse hepatocyte panel, enabling the *in vitro* early-stage prediction of drug-induced hepatocellular toxicity with consideration for a multi-genetic or multi-ethnic background. However, to mimic the pharmacokinetics in PM precisely, the model cells which do not have a deletion but have single nucleotide polymorphism (SNP) at the *CYP2C19* locus such as *CYP2C19**2 or *3 will be needed (Gardiner and Begg, 2006; Isomura *et al.*, 2010; Kiss *et al.*, 2018). Recently, genome editing technology that can introduce an SNP to human iPS cells has been developed (Kim *et al.*, 2018). Applying this technology, we would like to introduce (or correct) an SNP at the *CYP2C19* locus in human iPS cells, and then generate HLCs from the cells. In addition, new SNPs that affect the symptoms of PM could be discovered from the candidate SNPs identified by Genome-wide association studies (GWAS).

In this study, we established a hepatocyte model of CYP2C19-PMs and demonstrated its usefulness as a tool for drug discovery. We hope our technology contributes to the advance of CYP-PM studies, and to the safe and appropriate use of drugs for CYP-PMs.

DMD # 086322

Acknowledgement

We thank Ms. Yasuko Hagihara, Ms. Natsumi Mimura, and Ms. Ayaka Sakamoto for their excellent technical support.

DMD # 086322

Authorship Contributions

Participated in research design: Takayama

Conducted experiments: Deguchi, Igai, Harada, Takayama

Performed data analysis: Deguchi, Yamashita, Harada, Toba, Takayama

Wrote or contributed to the writing of the manuscript: Deguchi, Yamashita, Harada,

Hirata, Takayama, Mizuguchi

DMD # 086322

References

- Bertilsson L (1995) Geographical/Interracial Differences in Polymorphic Drug Oxidation. *Clin Pharmacokinet* **29**:192–209, Springer International Publishing.
- Gardiner SJ, and Begg EJ (2006) Pharmacogenetics, Drug-Metabolizing Enzymes, and Clinical Practice. *Pharmacol Rev*, doi: 10.1124/pr.58.3.6.
- Gillette M, Morneau K, Hoang V, Virani S, and Jneid H (2016) Antiplatelet Management for Coronary Heart Disease: Advances and Challenges. *Curr Atheroscler Rep* **18**:35, Springer US.
- Isomura Y, Yamaji Y, Ohta M, Seto M, Asaoka Y, Tanaka Y, Sasaki T, Nakai Y, Sasahira N, Hiroyuki •, Minoru Tada I•, Yoshida H, Kawabe T, Omata M, and Koike K (2010) A genetic polymorphism of CYP2C19 is associated with susceptibility to biliary tract cancer. *J Gastroenterol*, doi: 10.1007/s00535-010-0246-0.
- Kahma H, Filppula AM, Neuvonen M, Tarkiainen EK, Tornio A, Holmberg MT, Itkonen MK, Finel M, Neuvonen PJ, Niemi M, and Backman JT (2018) Clopidogrel carboxylic acid glucuronidation is mediated mainly by UGT2B7, UGT2B4, and UGT2B17: Implications for pharmacogenetics and drug-drug interactions. *Drug Metab Dispos* **46**:141–150.
- Kim S-I, Matsumoto T, Kagawa H, Nakamura M, Hirohata R, Ueno A, Ohishi M, Sakuma T, Soga T, Yamamoto T, and Woltjen K (2018) Microhomology-assisted scarless genome editing in human iPSCs. *Nat Commun* **9**:939, Nature Publishing Group.

DMD # 086322

- Kiss ÁF, Vaskó D, Déri MT, Tóth K, and Monostory K (2018) Combination of CYP2C19 genotype with non-genetic factors evoking phenoconversion improves phenotype prediction. *Pharmacol Reports* **70**:525–532, Institute of Pharmacology, Polish Academy of Sciences.
- Le C, Ann RF, David C, Lin S, Barretto R, Habib N, Hsu PD, Xuebing W, Jiang W, Marraffini LA, and Zhang F (2013) Multiplex Genome Engineering Using CRISPR/Cas Systems. *Science (80-)* **339**.
- Macdonald JS, and Robertson RT (2009) Toxicity Testing in the 21st Century: A View from the Pharmaceutical Industry. *Toxicol Sci* **110**:40–46.
- Nakamura K, Goto F, Ray WA, McAllister CB, Jacqz E, Wilkinson GR, and Branch RA (1985) Interethnic differences in genetic polymorphism of debrisoquin and mephenytoin hydroxylation between Japanese and Caucasian populations. *Clin Pharmacol Ther* **38**:402–408.
- Simon T, Verstuyft C, Mary-Krause M, Quteineh L, Drouet E, Méneveau N, Steg PG, Ferrières J, Danchin N, and Becquemont L (2009) Genetic Determinants of Response to Clopidogrel and Cardiovascular Events. *N Engl J Med* **360**:363–375.
- Stingl JC, Brockmöller J, and Viviani R (2013) Genetic variability of drug-metabolizing enzymes: the dual impact on psychiatric therapy and regulation of brain function. *Mol Psychiatry* **18**:273–287.
- Suzuki H, Kneller MB, Haining RL, Trager WF, and Rettie AE (2002) (+)-N-3-Benzyl-nirvanol and (-)-N-3-benzyl-phenobarbital: new potent and selective in vitro inhibitors of CYP2C19. *Drug Metab Dispos* **30**:235–9, American Society for

DMD # 086322

Pharmacology and Experimental Therapeutics.

Takayama K, Igai K, Hagihara Y, Hashimoto R, Hanawa M, Sakuma T, Tachibana M, Sakurai F, Yamamoto T, and Mizuguchi H (2017) Highly efficient biallelic genome editing of human ES/iPS cells using a CRISPR/Cas9 or TALEN system. *Nucleic Acids Res* **45**:5198–5207.

Takayama K, and Mizuguchi H (2017) Generation of human pluripotent stem cell-derived hepatocyte-like cells for drug toxicity screening. *Drug Metab Pharmacokinet* **32**:12–20, Elsevier Ltd.

Takayama K, Morisaki Y, Kuno S, Nagamoto Y, Harada K, Furukawa N, Ohtaka M, Nishimura K, Imagawa K, Sakurai F, Tachibana M, Sumazaki R, Noguchi E, Nakanishi M, Hirata K, Kawabata K, and Mizuguchi H (2014) Prediction of interindividual differences in hepatic functions and drug sensitivity by using human iPS-derived hepatocytes. *Proc Natl Acad Sci U S A* **111**:16772–16777.

Tsamandouras N, Chen WLK, Edington CD, Stokes CL, Griffith LG, and Cirit M (2017) Integrated Gut and Liver Microphysiological Systems for Quantitative In Vitro Pharmacokinetic Studies. *AAPS J* **19**:1499–1512, Springer US.

Wallentin L, James S, Storey RF, Armstrong M, Barratt BJ, Horrow J, Husted S, Katus H, Steg PG, Shah SH, and Becker RC (2010) Effect of CYP2C19 and ABCB1 single nucleotide polymorphisms on outcomes of treatment with ticagrelor versus clopidogrel for acute coronary syndromes: A genetic substudy of the PLATO trial. *Lancet* **376**:1320–1328, Elsevier Ltd.

Zahno A, Bouitbir J, Maseneni S, Lindinger PW, Brecht K, and Krähenbühl S (2013)

DMD # 086322

Hepatocellular toxicity of clopidogrel: Mechanisms and risk factors. *Free Radic Biol Med* **65**:208–216, Elsevier.

Zanger UM, and Schwab M (2013) Cytochrome P450 enzymes in drug metabolism: Regulation of gene expression, enzyme activities, and impact of genetic variation. *Pharmacol Ther* **138**:103–141, Pergamon.

Zhai Y, Wang L, Yang F, Feng G, Feng S, Cui T, An L, and He X (2016) The mechanism and risk factors of clopidogrel-induced liver injury. *Drug Chem Toxicol* **39**:367–374.

DMD # 086322

Footnotes

Financial support

This research is supported by the grants from Japan Agency for Medical Research and development, AMED (19mk0101125h0002, 19be0304320h0003).

Conflict of interest statement

The authors declare no competing financial interests.

Person to receive reprint requests

Dr. Kazuo Takayama

Laboratory of Biochemistry and Molecular Biology, Graduate School of Pharmaceutical Sciences, Osaka University, 1-6 Yamadaoka, Suita, Osaka 565-0871, Japan.

E-mail: takayama@phs.osaka-u.ac.jp

DMD # 086322

Figure legends

Figure 1 Generation of CYP2C19-knockout human iPS cells

(A) A schematic overview of the targeting strategy for *CYP2C19* is shown. PCR primers that can distinguish the wild type and mutant alleles are shown with arrows. The following donor plasmids were used to target the *CYP2C19* locus. Donor plasmids: EF1 α ; elongation factor 1 alpha promoter, PuroR; puromycin resistant protein, pA; polyadenylation sequence. The CRISPR-Cas9 system was applied to produce *CYP2C19* sequence-specific double strand breaks. (B) Genotyping was performed to examine whether the human iPS cell clones were correctly targeted.

Figure 2 Effect of CYP2C19 deficiency on the undifferentiated state

(A) Phase contrast images of WT iPSCs and CYP2C19-KO iPSCs are shown. Scale bars represent 500 μ m. (B) The gene expression levels of pluripotent markers (*NANOG*, *OCT3/4*, and *SOX2*) were measured by real time RT-PCR analysis in WT iPS cells and CYP2C19-KO iPS cells. The gene expression levels in undifferentiated WT iPS cells were taken as 1.0. (C) WT and CYP2C19-KO iPS cells were subjected to immunostaining with anti-OCT3/4 (green) and anti-SOX2 (red) antibodies. Nuclei were counterstained with DAPI (blue). Scale bars represent 100 μ m. All data are represented as means \pm SD ($n=3$). * $p<0.05$, ** $p<0.01$.

Figure 3 Hepatic differentiation capacity of CYP2C19-knockout human iPS cells

Human iPS cells (FCL-iPS) were differentiated into the HLCs as described in the Materials and Methods section. (A) The schematic overview shows the protocol for hepatic differentiation. (B) The gene expression levels of hepatocyte markers (*ALB*, *AFP*,

DMD # 086322

AAT, *TTR*, *HNF4A*, and *CYP3A4*) were examined in undifferentiated WT iPS cells, undifferentiated CYP2C19-KO iPS cells, WT iPS cell- and CYP2C19-KO iPS cell-derived HLCs by real-time RT-PCR. The gene expression levels in WT iPS cell-derived HLCs were taken as 1.0. (C) The amounts of ALB secretion were examined in WT iPS cell- and CYP2C19-KO iPS cell-derived HLCs by ELISA. (D) The expression of the hepatocyte markers (ALB and *AAT*) in human iPS cell-derived HLCs was examined by immunohistochemistry. Nuclei were counterstained with DAPI (blue). Scale bars represent 50 μ m. All data are represented as means \pm SD ($n=3$). * $p<0.05$, ** $p<0.01$.

Figure 4 Transcriptomic analysis of CYP2C19-knockout human iPS cell-derived hepatocyte-like cells

Human iPS cells (FCL-iPS) were differentiated into the HLCs as described in the Materials and Methods section, and then the cells were analyzed by DNA microarray. A scatter plot of the gene expression signals in WT HLCs and CYP2C19-KO HLCs is shown. Red dots and blue dots indicate the genes whose expression levels were up- and down-regulated more than 3-fold, respectively.

Figure 5 Drug metabolism capacity of CYP2C19-knockout human iPS cell-derived hepatocyte-like cells

Human iPS cells (FCL-iPS) were differentiated into the HLCs as described in the Materials and Methods section. The CYP-mediated drug metabolizing capacities in WT iPS cell- and CYP2C19-KO iPS cell-derived HLCs were evaluated by quantifying the metabolites of CYP substrates (*S*-mephenytoin; substrate for CYP2C19). The quantity of metabolites (4'-hydroxymephenytoin) was measured by UPLC-MS/MS. The results are

DMD # 086322

shown as means \pm SD ($n = 6$). Statistical significance was evaluated by unpaired two-tailed Student's t -tests (** $p < 0.01$).

Figure 6 Drug response of CYP2C19-knockout human iPS cell-derived hepatocyte-like cells

Human iPS cells (FCL-iPS) were differentiated into the HLCs as described in the Materials and Methods section. The cell viability of WT iPS cell- and CYP2C19-KO iPS cell-derived HLCs was assessed by WST-8 assay after 48 hr exposure to different concentrations of clopidogrel. The cell viability was calculated as a percentage of cells treated with solvent only. The results are shown as means \pm SD ($n = 3$).

Figure 7 Drug response of ketoconazole-treated CYP2C19-knockout human iPS cell-derived hepatocyte-like cells

Human iPS cells (FCL-iPS) were differentiated into the HLCs as described in the Materials and Methods section. The HLCs were treated with ketoconazole (a CYP3A4 inhibitor) for 48 hr. The cell viability of WT iPS cell- and CYP2C19-KO iPS cell-derived HLCs was assessed by WST-8 assay after 48 hr exposure to different concentrations of clopidogrel. The cell viability was calculated as a percentage of cells treated with solvent only. The results are shown as means \pm SD ($n = 3$). Statistical significance was evaluated by one-way ANOVA followed by Bonferroni's post-hoc tests (** $p < 0.01$: compared with "vehicle").

Figures

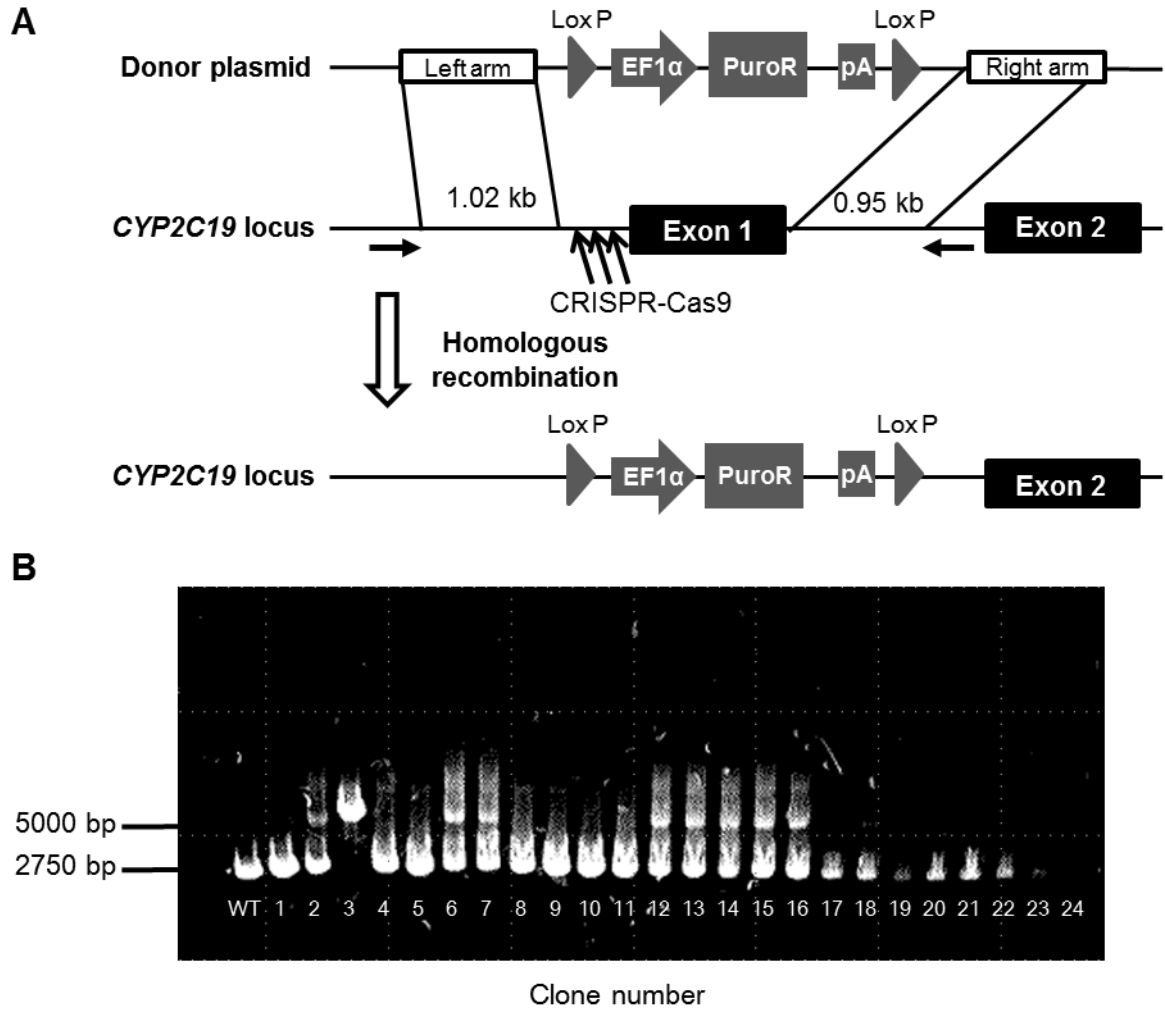


Figure 1

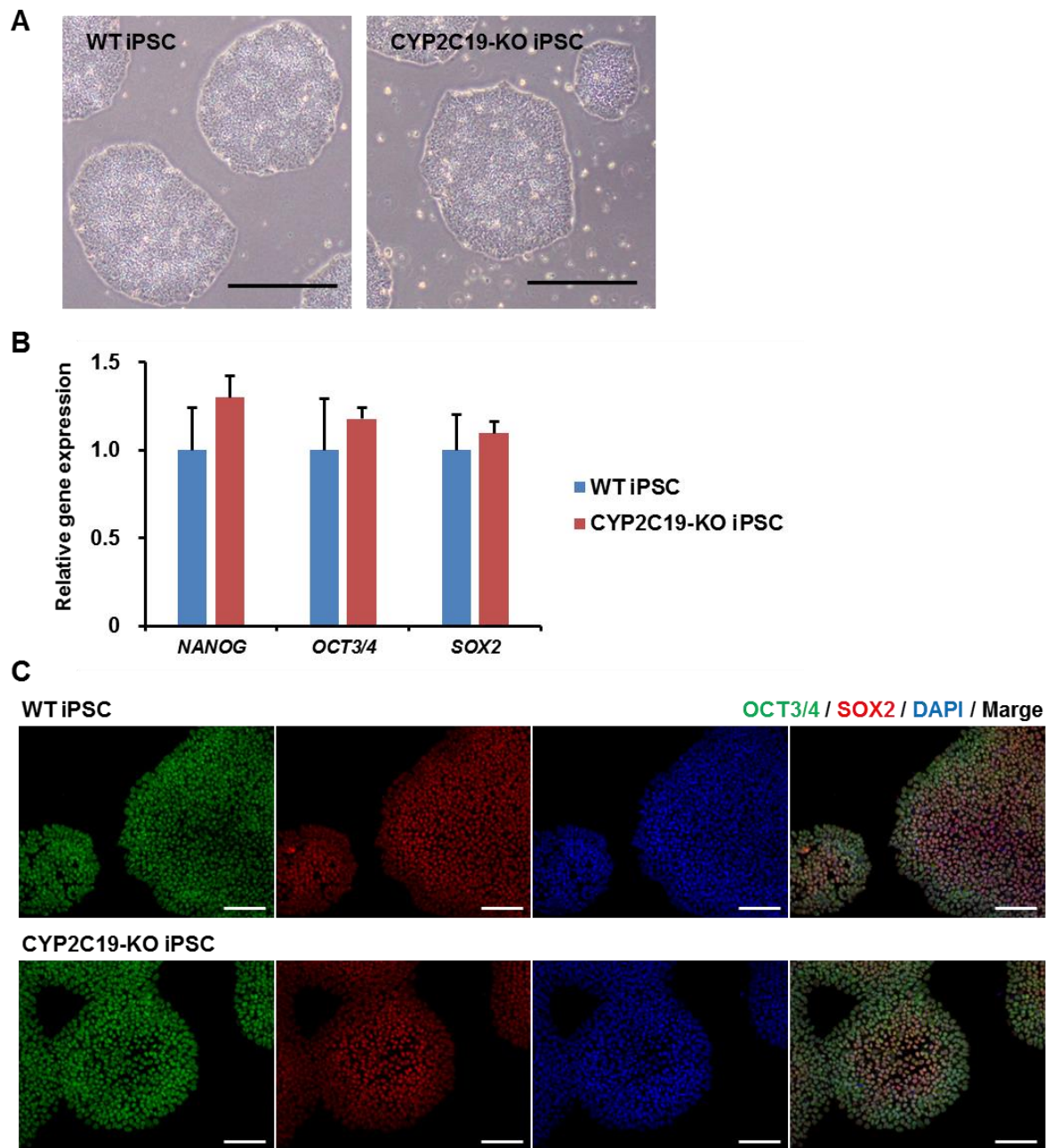


Figure 2

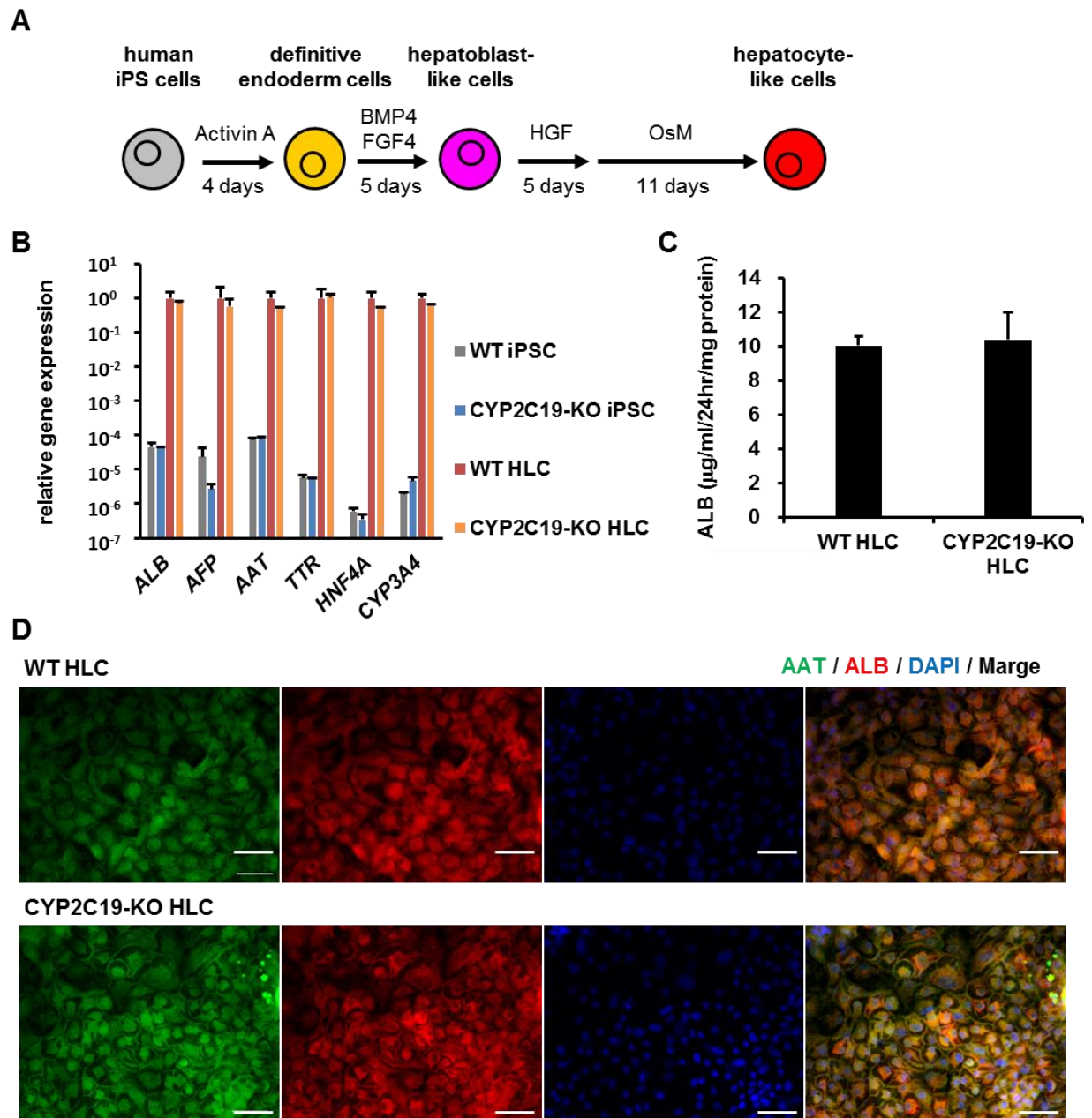
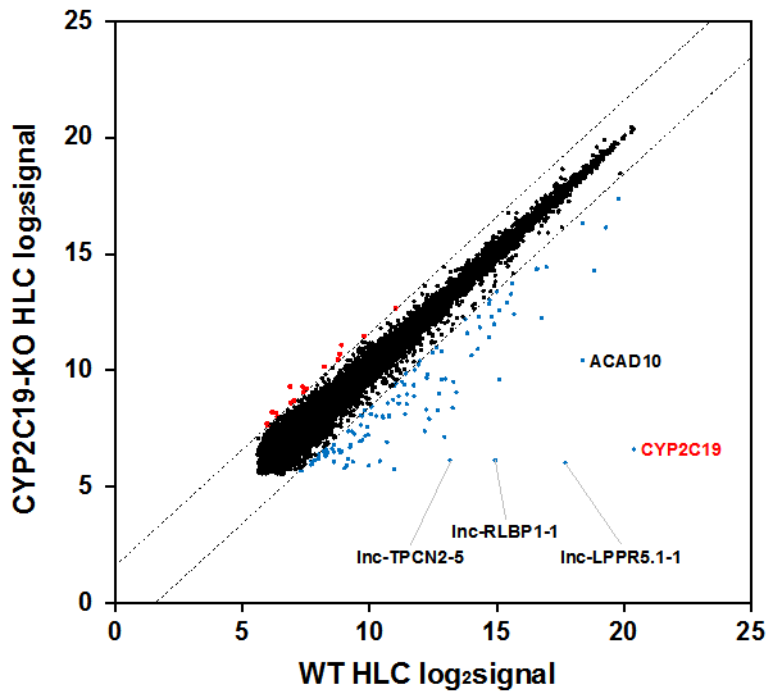


Figure 3



Dot	Description	Count	Rate
	Detected	27331	100 %
●	Up-regulated > 3-fold	18	0.07 %
●	No change	27197	99.5 %
●	Down-regulated > 3-fold	116	0.43 %

Figure 4

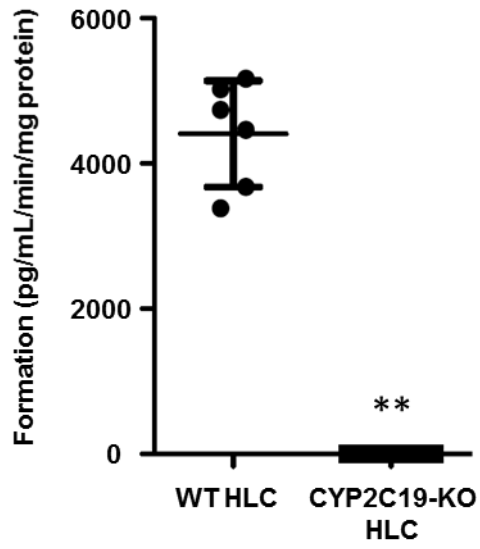


Figure 5

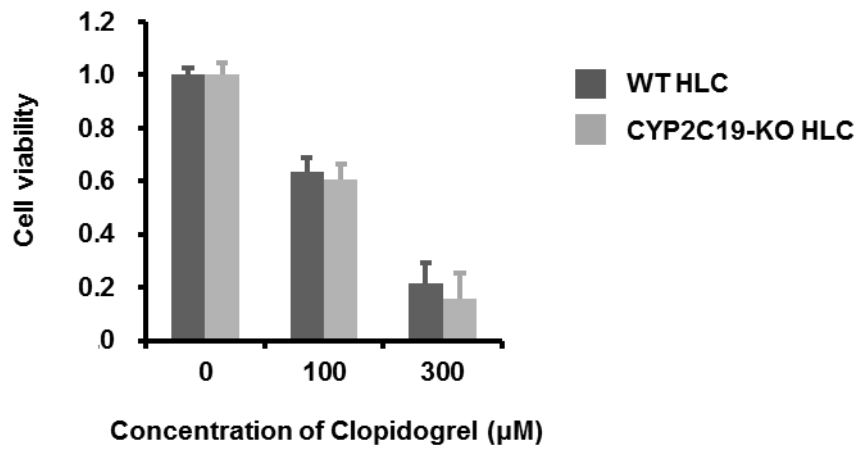


Figure 6

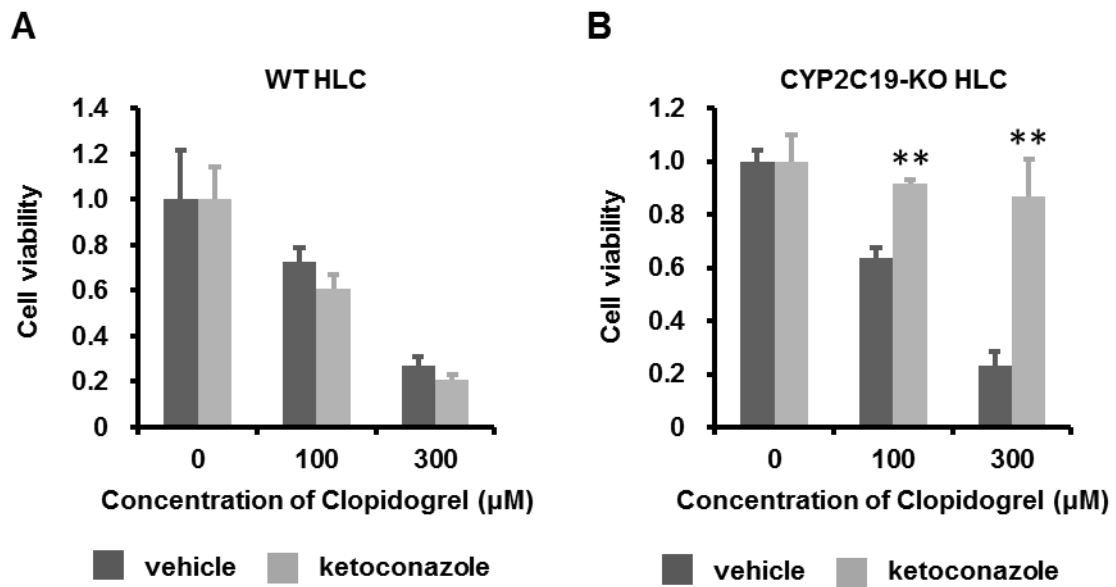


Figure 7